Experimental and simulated fast ion velocity distributions on collective Thomson scattering diagnostic in the Large Helical Device

M. Nishiura, S. Kubo, K. Tanaka, R. Seki, T. Shimozuma, T. Mutoh, K. Kawahata, T. Watari, S. Ogasawara, T. Saito[a], Y. Tatematsu[a], S. B. Korsholm[b], F. Meo[b], M. Stejner[b], M. Salewski[b], S. Murakami[c], H. Yamaguchi[c], LHD experiment group

National Institute for Fusion Science,322-6 Oroshi-cho, Toki 509-5292, Japan

[a]FIR FU, University of Fukui, 3-9-1 Bunkyo, Fukui, 910-8507, Japan

[b]Risø National Laboratory, Technical University of Denmark, 4000 Roskilde, Denmark

[c]Department of Nuclear Engineering, Kyoto University, Kyoto 606-8501, Japan

Introduction

It is essential to understand the behavior of charged fusion products and related physics in burning plasmas. For diagnosing them in the plasma core region, one of choices is to employ an electromagnetic wave and their scattering. The collective Thomson scattering (CTS) technique has been developed using a high power and GHz gyrotron in fusion devices such as JET, W7-AS, TEXTOR, and ASDEX Upgrade [1-5] and designed for ITER [3, 5].

We have developed a CTS apparatus to measure bulk and fast ions in the Large Helical Device (LHD) [6-8]. The observed CTS spectra have to be compared quantitatively with the modeled spectrum to obtain the fast ion velocity distribution. As the first step, we have calculated the electromagnetic fluctuation for the CTS spectrum with Maxwellian or slowing down distribution. The 1D model is valid only for the isotropic velocity distribution, and we must consider an anisotropic one for practical plasmas, i.e. tangential neutral beam injected plasmas. The measured CTS signal is evaluated from the 1D velocity distribution, where the particles on the velocity space ($v_{||}$, $v_{\perp}$) are projected onto the fluctuation wave vector $\boldsymbol{k}^{\delta}$(= $\boldsymbol{k}^{s}$ – $\boldsymbol{k}^{i}$). Thus the observed CTS spectrum is sensitive strongly to the $\boldsymbol{k}^{\delta}$ direction. The spectrum results in a distorted shape, in particular, when the fast ions become an anisotropic velocity distribution due to an auxiliary beam. The geometrical and anisotropic effects for CTS diagnostics are discussed [9]. In the case of our experiments, GNET code [10] and an orbit following Monte-Carlo code (MORH) [11], which simulate the fast ion behavior in LHD plasmas, give us the fast ion velocity distribution on the ($v_{||}$, $v_{\perp}$) space at a time frame. From these simulated results the expected CTS spectra are calculated numerically as the same manner as the reference [9], and can be compared with the experimental one.

Experimental setup and CTS spectrum measurement

The scattered radiation from the cross volume on the probing and the receiving beams are collected by a steering mirror for ECH, and it is through a transmission line to the CTS receiver front end. The CTS broad band receiver of a heterodyne system is shown in Fig.1. The receiver consists of mainly a notch filter for the rejection of a gyrotron stray light, a mixer with a local oscillator, and intermediate frequency (IF) amplifiers and diodes. The diode output is amplified by 100 times at the video amplifiers. The broad band receiver resolves the scattered signal into 32 channels. These signals are stored into the LHD database with a sampling rate of a hundred kHz. The sensitivity of the CTS receiver channels is calibrated by using the radiation from liquid nitrogen or an electron cyclotron emission combined with electron temperatures of non-collective Thomson scattering diagnostic. These calibration factors are relatively agreement with each other in both cases.

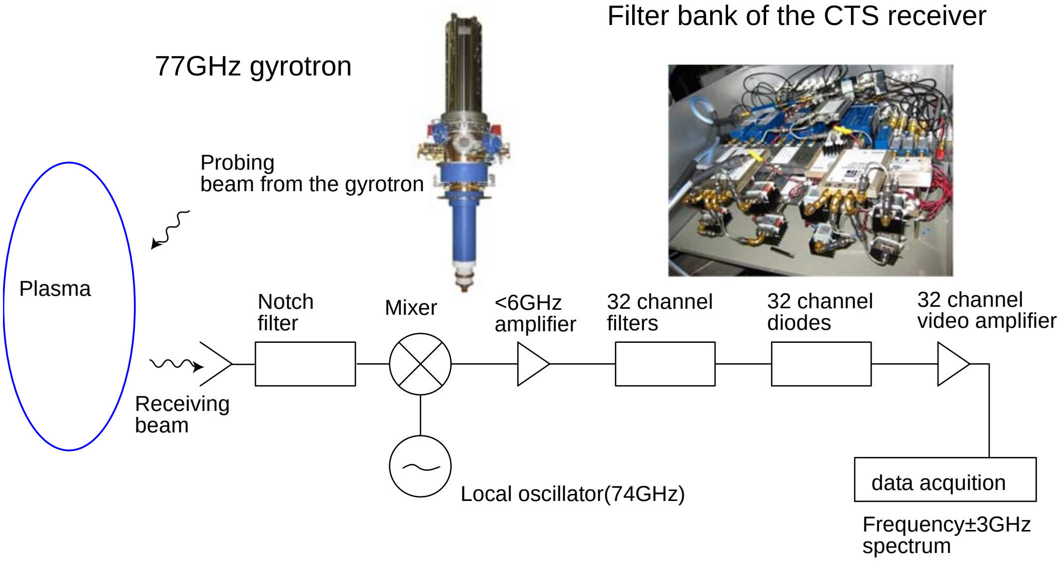

Fig. 1. Schematic diagram of the CTS broad band receiver system. The probing beam of 77GHz gyrotron is used.

The probing beam from a 77 GHz gyrotron is modulated with 50 Hz to subtract the background electron cyclotron emission (ECE) from the detected signals. The scattered signals for both ON and OFF timings are averaged over 1 ms before and after the trailing edge. Fig. 2 shows the CTS spectrogram and the CTS spectra at specific times. The excited wave in the lower hybrid range is observed during the injection of the perpendicular NB4 in this discharge. The characteristics of excited wave are reported in the reference [8]. Here we discuss the fast ion velocity distribution compared with the simulated one. The angle between the wave vector and the magnetic field $\angle(\boldsymbol{k}^{\delta}, \boldsymbol{B})$ is 100.4 degrees in this experiment. The MORH code shows that the fast ion density is of the order of $10^{17}\mathrm{m}^{-3}$, which are two orders of magnitude lower than the bulk ion density. The measured intensity of CTS spectra should be a similar ratio of bulk to fast ion densities. The detection of the signal level is severe because of the competition with the background ECE.

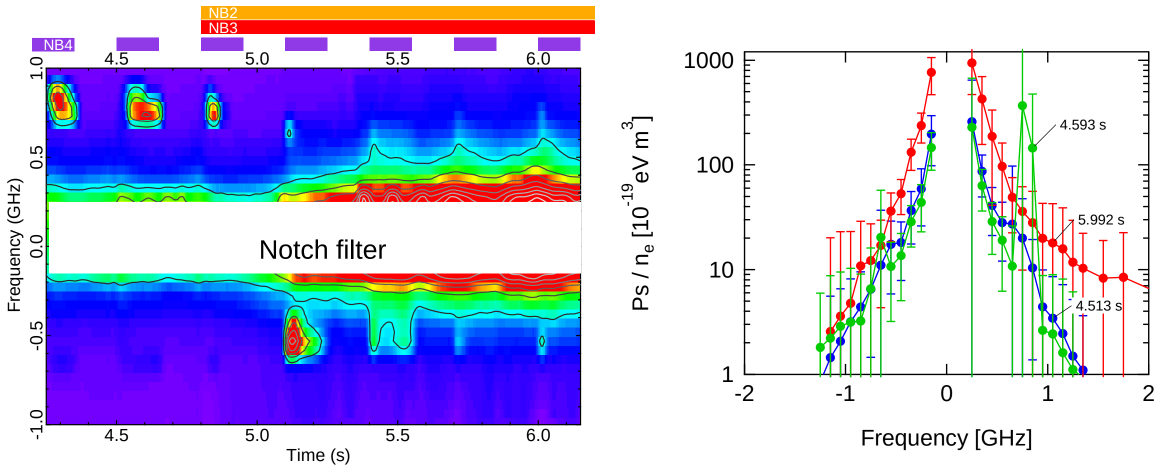

Fig. 2. Measured CTS spectrogram with neutral beam injections. The direction of NBs in LHD is described in Fig.2. The CTS spectra at different NB injection timing for (1) t=4.513s, (2) t=4.593s, and (3) t=5.992s. The beam energies are ~170keV for NB1 to 3, and ~40 keV for NB4.

The comparative study between experiment and simulation has been carried out to understand the CTS spectrum as well as code prediction for fast ion confinement. Fig. 3 shows that the fast ion velocity distribution on the velocity space ($v_{\|}$, $v_{\perp}$), which is calculated by the MORH code at t = 6.0 s. In this case, two parallel and one perpendicular beams are

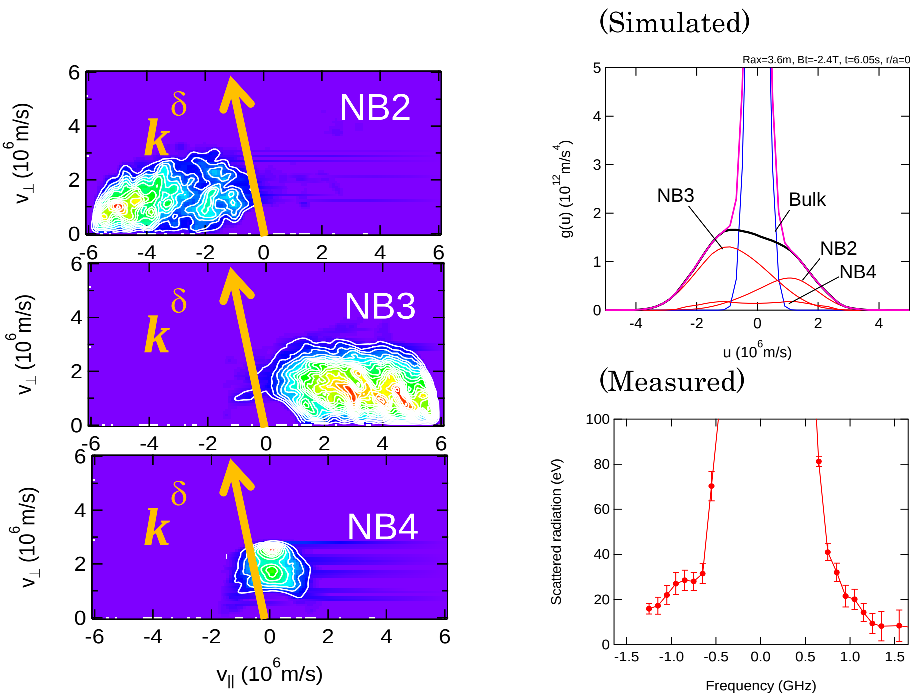

Fig. 3. Simulated fast ion distribution during NB#2, NB#3, and NB#4 injections by the MORH code. The right graph is the 1D velocity distribution calculated from the left figures with the k^{δ} vector of 100 degrees.

injected. The observation direction is the angle of 100 degrees as the $\boldsymbol{k}^{\delta}$ vector is indicated in the figure. Therefore all particles are projected onto the $\boldsymbol{k}^{\delta}$ vector. After the treatment of this geometrical effect, we can obtain the one dimensional velocity distribution in the right graph of Fig. 3. We found that the total 1D velocity distribution is dominated by the parallel fast ions originated from NB2 and NB3 rather than NB4. From Fig. 3, the measured CTS spectrum at less than -0.7 GHz and more than 0.7 GHz is considered to be these fast ions.

At the same sightline near perpendicular direction, when only perpendicularly particles with the energy of ~40 keV are injected at t = 0.451 s, the simulated CTS spectrum becomes a symmetrical shape. On the other hand, even if the sightline is near perpendicular direction, tangentially injected particles with the energy of ~180 keV would affect the CTS spectra, and they become the asymmetrically 1D velocity distribution function. For more detail discussion, we will evaluate the CTS spectrum with using the simulated 1D velocity distribution for the comparison between the measured and the simulated spectra.

Summary

We have developed a collective Thomson scattering diagnostic system in the LHD. The CTS spectrum spread is observed in the frequency region corresponding to the bulk and fast ions during NB injection. The NB originated fast ions are evaluated by the MORH code for understanding the measured CTS spectra. We found that tangentially injected particles affect the CTS spectrum in the fast ion region from the simulated 1D velocity distribution for fast ions. This is consistent with the measured CTS spectrum in the frequency shift at less than -0.7 GHz and more than 0.7 GHz. As the next step, the CTS spectrum would be evaluated using the simulated 1D velocity distribution.

Acknowledgment

This work is supported by Grant-in-Aid for Scientific Research(B)#21360455 and #24360385.

References

[1] H. Bindslev, J. A. Hoekzema, J. Egedal *et al*., Phys. Rev. Lett. **83**, 3206(1999).
[2] E. V. Suvorov, V. Erckmann, E. Holzhauer *et al*., Plasma Phys. Control Fusion **37**, 1207(1995).
[3] S. B. Korsholm, H. Bindslev, F. Meo *et al*., Rev. Sci. Instrum. 77, 10E514(2006).
[4] M. Salewski, F. Meo, M. Stejner *et al*., Nucl. Fusion **50**, 035012(2010).
[5] F. Meo, H. Bindslev, S. B. Korsholm *et al*., Rev. Sci. Instrum. **75**, 3585(2004).
[6] S. Kubo, M. Nishiura, K. Tanaka *et al*., Rev. Sci. Instrum. **81**, 10D535(2010).
[7] Y. Tatematsu, S. Kubo, M. Nishiura *et al*., 23rd IAEA Fusion Energy Conference 2010, FTP/P6-31.
[8] M. Nishiura, S. Kubo, K. Tanaka et al., Plasma and Fusion Res. **6**, 2402068(2011).
[9] M. Salewski, S. K. Nielsen, H. Bindslev, V. Furtula, et al., Nucl. Fusion **51**, 083014(2011).
[10] S. Murakami *et al*., Fusion Sci. Technol. 46 (2004) 241.
[11] Ryosuke Seki, Yutaka Matsumoto, Yasuhiro Suzuki, Kiyomasa Watanabe, Kiyotaka Hamamatsu, Masafumi Itagaki, Plasma and Fusion Research, Vol. 5, 027(2010).